SUPPLEMENTARY MATERIAL

Title: Climatic similarity and genomic background shape the extent of parallel adaptation in *Timema* stick insects

Short title: Parallel adaptation to climate

Samridhi Chaturvedi[1,2*], Zachariah Gompert[2*], Jeffrey L. Feder[3], Owen G. Osborne[4], Moritz Muschick[5,6], Rüdiger Riesch[7], Víctor Soria-Carrasco[8] and Patrik Nosil[2,9]

[1]Department of Integrative Biology, University of California, Berkeley, California 94703 USA
[2]Department of Biology and Ecology Center, Utah State University, Logan, Utah 84322, USA
[3]Department of Biological Sciences, University of Notre Dame, Notre Dame, Indiana 46556, USA
[4]Molecular Ecology and Evolution Bangor, Environment Centre Wales, School of Natural Sciences, Bangor University, Bangor, LL57 2UW, UK
[5]Aquatic Ecology & Evolution, Institute of Ecology and Evolution, University of Bern, CH-3012, Switzerland
[6]Department of Fish Ecology & Evolution, Eawag, Swiss Federal Institute for Aquatic Science and Technology, CH-6047, Kastanienbaum, Switzerland
[7]Department of Biological Sciences, Royal Holloway University of London, Egham, TW20 9EX, UK
[8]The John Ines Center, Norwich Research Park, Norwich, NR4 7UH, UK
[9]CEFE, Univ Montpellier, CNRS, EPHE, IRD, Univ Paul Valéry Montpellier 3, Montpellier, France
*Corresponding authors (Emails: Samridhi Chaturvedi – samridhi.chaturvedi@gmail.com; Zachariah Gompert – zach.gompert@usu.edu)

SUPPLEMENTARY METHODS

Climate-associated SNP windows and cuticular hydrocarbon variation

We tested for excess overlap between climate-associated SNP windows and genomic regions associated with cuticular hydrocarbon (CHC) variation. The logic here is that CHCs often play a role in desiccation tolerance and climatic adaptation in insects (e.g., [1]), such that genetic regions associated with climate versus CHCs might overlap. We thus specifically quantified the extent to which climate-associated SNP windows overlapped with windows harboring SNPs associated with CHCs, and whether this overlap was greater than expected by chance. The CHC data were originally described and analyzed by [2]. Specifically, for each insect, we had quantified the proportional abundance of 26 different mono- and di-methylated CHCs, which comprised eight pentacosanes, eight heptacosanes and ten nonacosanes, and then applied log-

contrasts. For the current dataset, we used those values to calculate the proportional abundance of the sum of all pentacosanes, the sum of all heptacosanes and the sum of all nonacosanes (henceforth: pentacosanes, heptacosanes and nonacosanes). Therefore, the six CHC traits considered were pentacosanes, heptacosanes, and nonacosanes in males and females (i.e., three molecule types in each of two sexes = six traits total).

Here, we first re-aligned the GBS data from [2] to the current (i.e., more recent and less fragmented) *T. cristinae* genome (draft version 0.3). This included GBS data from 395 male and 195 female *T. cristinae* all collected from a single population (FHA), and all of which for CHC data was also collected. These data were aligned to the genome using the BWA ALN algorithm (version 0.7.17-r1188) [4]. We allowed for 5 mismatches total, and not more than 2 miss-matches in the first 20 bp. Only reads with a mapping quality greater than 10 were retained. We then compressed, sorted, and indexed the alignments with SAMTOOLS and BCFTOOLS (version 1.2) [5,6]. Next, we used SAMTOOLS and BCFTOOLS to identify SNPs and calculate genotype likelihoods. For this, we used the recommended mapping quality adjustment (-C 50), only considered alignments with mapping qualities of 20 or more and SNPs with base qualities of 30 or more, and only called variants when the posterior probability that the locus was invariant was less than 0.01 given a prior mutation rate parameter of 0.001. We then used custom Perl scripts to filter out variants with a mean coverage of less than 2x, fewer than 10 non-reference reads total, mapping quality less than 30, minor allele frequency less than ~0.005, more than 1% of reads in the reverse orientation (with our GBS method, all reads should have the same orientation), missing data (no reads) for more than 20% of individuals, SNPs with more than two alleles, and SNPs with coverage exceeding three standard deviations above the mean. Finally, we obtained Bayesian point estimates (posterior means) of genotypes for each locus and individual based on the genotype likelihoods and used the estimated allele frequencies to parameterize a binomial prior.

We then conducted genetic mapping of CHC variation using a polygenic genome-wide association (GWA) mapping approach, that controls for linkage disequilibrium among SNPs and background population structure as detailed below. We specifically fit Bayesian sparse linear mixed models (BSLMMs) to determine the contribution of additive genetic variation (as captured by our collective SNP data set) to each of six CHC traits, and to determine the

probability of association (posterior inclusion probability, PIP) of each individual SNP with each trait (this PIP value is computed from, i.e., equal to, the proportion of MCMC samples that included each SNP in the polygenic regression model). We fit this model using gemma (version 0.95a) [7], a polygenic GWA mapping method that fits a single model with all SNPs while accounting for uncertainty and redundancy in genotype-phenotype associations, for example by controlling for linkage disequilibrium among SNPs, and background polygenic effects. The latter is inferred based on a kinship matrix derived from the collective SNPs, which also serves to control for population structure when estimating effects for individual SNPs. Models were fit using MCMC, with each mapping exercise involving 10 independent chains each comprising 1 million sampling iterations and a 200,000-iteration burn-in.

Based on these analyses, we then computed the mean posterior inclusion probability or PIP (i.e., probability of a genotype-phenotype association) across all SNPs in 100 Kb windows for each of the six CHC traits. Then, we asked whether the average association with CHCs (averaged over windows) was higher for the climate-associated SNP windows than expected by chance. Randomisations (1000) were used to generate a null distribution. Specifically, mean posterior probabilities for SNP-CHC associations were permuted across 1000 Kb windows and the number windows in the top 10% for climate association and (permuted) CHC posterior inclusion probabilities was determined. Note that we conducted this test independently for each of the six CHC traits and each of the three climate PCs. We then examined the combination of these results to assess the total evidence that SNP windows associated with climate adaptation are enriched for those regions of the genome possibly affecting CHC variation.

Identifying introgression and population structure

We quantified both historical and contemporary gene flow patterns, respectively as follows. For identifying historical introgression, we used TREEMIX (version 1.13) [8] to construct a population-based phylogeny to identify historical admixture or gene flow among our 53 focal populations. This differed from previous TREEMIX analysis done for *Timema* species where we used the data only from the *Mel-Stripe* locus [3]. For the analysis in our study here, we re-aligned the GBS sequences for 1420 individuals (across 53 populations) included in this study to the *T. cristinae* genome (draft version 0.3). We did this by using the MEM algorithm from BWA (version 0.7.17-r1188). We ran BWA MEM with a minimum seed length of 15, internal seeds of

longer than 20 bp, and only output alignments with a quality score >= 30. We then used SAMTOOLS (version 1.6) to compress, sort and index the alignments [5,6]. We then identified SNPs using SAMTOOLS and BCFTOOLS (version 1.6). For variant calling, we used a mapping quality of 50, skipped alignments with mapping quality lower than < 20, skipped bases with base quality <15, and ignored insertion-deletion polymorphisms. We set the prior on SNPs to 0.001 and called SNPs when the posterior probability that the nucleotide was invariant was <=0.01. After we got the initial set of variants, we filtered them to retain only those SNPs with sequence data for at least 80% individuals, a mean sequence depth of two per individual, at least 4 reads of the alternative allele, a minimum quality score of 30, a minimum overall minor allele frequency of at least 0.005, and no more than 1% of the reads in the reverse orientation (this is an expectation for our GBS method). We further removed SNPs with excessive coverage (3 standard deviations above the mean) or that were tightly clustered (within 3 bp of each other), as these could be poor alignments (e.g., reads from multiple paralogs mapping to the same region of the genome). This left us with 8787 SNPs for this analysis. We used custom perl scripts to calculate genotype likelihoods for these SNPs and then used expectation-maximization algorithm to obtain maximum-likelihood estimates of population allele frequencies while accounting for uncertainty in genotypes (based on the calculated genotype likelihoods from BCFTOOLS). Finally, we used TREEMIX to construct *Timema* population graphs based on the matrix of allele frequency covariance between pairs of populations. We fit trees allowing 0-9 admixture events and calculate the proportion of variance in allele frequency variances explained by the population tree with the varying numbers of admixture events. This way we could determine the extent to which individual admixture events improved model fit.

For estimating contemporary gene flow, we implemented the admixture model from ENTROPY (version 1.2) [9]. This analysis yielded similar results as previously reported using the same model [2]. From ENTROPY, we obtained Bayesian estimates of genotypes and admixture proportions. This analysis was performed separately for each species- and species-specific set of SNPs. We did this to identify contemporary gene flow within species to understand if gene flow could affect parallelism in response to climate. The admixture model in ENTROPY is similar to that in STRUCTURE [10] but differs by accounting for uncertainty in genotypes arising from finite sequence coverage and sequence errors, and by allowing simultaneous estimation of

genotypes and admixture proportions. For each species, we fit the model with $k \in \{2\ldots5\}$ source populations. For each value of k, we ran three MCMC chains, each with 8000 iterations, a burn-in of 5000 iterations and a thinning interval of 3. We used assignments from a discriminant analysis of principal components to initialize the MCMC algorithm; this speeds convergence to the posterior and avoids label switching during MCMC without affecting the posterior probability distribution. We obtained genotype estimates as the posterior mean allele count for each individual and locus across chains and values of k (i.e., this integrates over uncertainty in the number of hypothetical source populations). We summarized patterns of population structure and admixture across the sampled populations and individuals based on these admixture proportions for k=2 and a principal component analysis (PCA) of the genotypic data. We then used the prcomp function [11] to perform a PCA in R (3.4) on the centered, but unstandardized genotype matrix.

SUPPLEMENTARY RESULTS

Climate-associated SNP windows and CHCs

In addition to the test for natural selection using the field experiment, we conducted additional tests using genetic mapping of cuticular hydrocarbons (CHCs) in *Timema cristinae*. For the CHC analyses, we considered three compound classes - pentacosanes, heptacosanes, and nonacosanes - in males and in females (i.e., three compounds x two sexes = six CHC traits total). We found evidence of heritable variation for each compound in both male and female *T. cristinae*, with 50.8% (male nonacosanes) to 89.7% (female pentacosanes) of the variability in these traits explained by a total of ~176 thousand sequenced SNPs in a mapping population (these values denote Bayesian point estimates based on 602 *T. cristinae* from a single population, FHA) (see Supplementary Table 5 for details). We summarized the evidence that each 100 Kb window included CHC-associated SNPs by computing the mean posterior probability of association (i.e., the mean probability of a non-zero genotype-phenotype association, also known as the posterior inclusion probability or PIP) across SNPs in the same 100 Kb windows used for summarizing SNP-climate associations. Based on a randomisation test, we found that for some CHC traits the average posterior inclusion probability for SNPs in the top climate-associated SNP windows in *T. cristinae* was marginally but significantly greater than expected by chance. Specifically, the

average probability of SNPs being associated with female pentacosanes was ~1.05 times higher than expected by chance for both the top 10% of PC2 and PC3 climate-associated SNP windows (*P*-value = 0.009 for PC2 and *P*-value = 0.010 for PC3 based on 1000 permutations; Supplementary Tables 7 and 8). We also detected a marginally non-significant increase in the average posterior inclusion probability for SNP associations with female nonacosanes in the top 10% of PC3 climate-associated SNP windows (x-fold increase in mean inclusion probability = 1.03, *P*-value = 0.051, 1000 permutations, Supplementary Table 8). We did not detect any significant overlap of SNPs associated with CHCs and those associated with PC1 climate windows (Supplementary Table 6). These results for CHCs support the hypothesis that at least a subset of the top climate-associated SNP windows is associated with traits involved in climatic adaptation in *Timema*.

Introgression does not contribute to parallel evolution

We conducted two analyses, focused on different time scales, to ask if introgression and gene flow between species promotes gene sharing and thus climate-associated parallel evolution. First, we identified historical patterns of introgression using a population tree-based approach. Second, we identified contemporary patterns of gene flow using an admixture model. Both these analyses helped us to assess the degree of genetic independence in adaptation to climate within each species.

To identify historical patterns of introgression, we used TREEMIX to generate a tree for all populations and species, allowing for historical admixture or gene flow among intra-specific or inter-specific populations. For this analysis, we realigned GBS sequence data for all 1420 individuals included in this study to the *T. cristinae* genome. We then called and filtered single nucleotide polymorphisms (SNPs) to identify a final set of 8787 SNPs for the TREEMIX analysis. Our results from TREEMIX yielded a population graph or bifurcating tree depicting relationships between focal localities in the study. The best bifurcating tree explained 99.6% of the variation in the population allele-frequency covariances. In this tree, *Timema* populations formed eight major clades that grouped populations by species (Figure 5A). Adding migration edges to the tree increased the variance explained by a negligible extent (Supplementary Table 9), as expected given that the tree with no migration edges explained the overwhelming majority of the variation in the data. These results are consistent with two previous findings that little to

no evidence for introgression was observed in analogous analyses focused on the *Mel-Stripe* locus and that divergence times for the eight species in the current study ranged between 10 – 30 million years, which indicates that *Timema* represent an old radiation [3].

We further used the admixture model from ENTROPY (version 1.2) to infer contemporary gene flow (see methods for details). Here, we focused our analyses on pairs of species and, thus, on admixture proportions for k=2 to identify individuals of possible hybrid ancestry. We summarized patterns of population structure and admixture across the sampled populations and individuals based on these admixture proportions in principal component analyses (PCA) of the genotypic data (Supplementary Figures 7-9). As previously reported [2], we detected minimal evidence for contemporary admixture between species in the ENTROPY analysis. Together these results imply that introgression and gene flow do not strongly or regularly influence the dynamics of parallel adaptation to climate in these species.

SUPPLEMENTARY CITATIONS

1. Rajpurohit, S., R. Hanus, V. Vrkoslav, E. L. Behrman, A. O. Bergland, D. Petrov, J. Cvačka, and P. S. Schmidt. 2017. "Adaptive Dynamics of Cuticular Hydrocarbons in Drosophila." *Journal of Evolutionary Biology* 30 (1): 66–80.
2. Riesch, Rüdiger, Moritz Muschick, Dorothea Lindtke, Romain Villoutreix, Aaron A. Comeault, Timothy E. Farkas, Kay Lucek, et al. 2017. "Transitions between Phases of Genomic Differentiation during Stick-Insect Speciation." *Nature Ecology & Evolution* 1 (4): 82.
3. Villoutreix, Romain, Clarissa F. de Carvalho, Víctor Soria-Carrasco, Dorothea Lindtke, Marisol De-la-Mora, Moritz Muschick, Jeffrey L. Feder, Thomas L. Parchman, Zach Gompert, and Patrik Nosil. 2020. "Large-Scale Mutation in the Evolution of a Gene Complex for Cryptic Coloration." *Science (New York, N.Y.)* 369 (6502): 460–66.
4. Li, Heng. 2013. "Aligning Sequence Reads, Clone Sequences and Assembly Contigs with BWA-MEM." *ArXiv [q-Bio.GN]*. arXiv. http://arxiv.org/abs/1303.3997.
5. Li, Heng, Bob Handsaker, Alec Wysoker, Tim Fennell, Jue Ruan, Nils Homer, Gabor Marth, Goncalo Abecasis, Richard Durbin, and 1000 Genome Project Data Processing Subgroup. 2009. "The Sequence Alignment/Map Format and SAMtools." *Bioinformatics (Oxford, England)* 25 (16): 2078–79.
6. Danecek, Petr, James K. Bonfield, Jennifer Liddle, John Marshall, Valeriu Ohan, Martin O. Pollard, Andrew Whitwham, et al. 2021. "Twelve Years of SAMtools and BCFtools." GigaScience 10 (2). https://doi.org/10.1093/gigascience/giab008.
7. Zhou, Xiang, Peter Carbonetto, and Matthew Stephens. 2013. "Polygenic Modeling with Bayesian Sparse Linear Mixed Models." *PLoS Genetics* 9 (2): e1003264.
8. Pickrell, Joseph K., and Jonathan K. Pritchard. 2012. "Inference of Population Splits and Mixtures from Genome-Wide Allele Frequency Data." *PLoS Genetics* 8 (11): e1002967.
9. Gompert, Zachariah, Lauren K. Lucas, C. Alex Buerkle, Matthew L. Forister, James A. Fordyce, and Chris C. Nice. 2014. "Admixture and the Organization of Genetic Diversity in a Butterfly Species Complex Revealed through Common and Rare Genetic Variants." *Molecular Ecology* 23 (18): 4555–73.
10. Pritchard, J. K., M. Stephens, and P. Donnelly. 2000. "Inference of Population Structure Using Multilocus Genotype Data." *Genetics* 155 (2): 945–59.
11. Kassambara, Alboukadel. 2019. *Practical Statistics in R for Comparing Groups*. Practical Statistics in R 2. Independently Published.

SUPPLEMENTARY TABLES

Supplementary Table 1: Locality information and sample sizes for the eight species and 53 localities for which the GBS data has been included in this study. The GBS data associated with these populations and individuals was first presented in [2].

Species	**No. of populations**	**No. of individuals**
T. bartmani	6	195
T. californicum	3	77
T. chumash	12	358
T. cristinae	6	205
T. knulli	5	89
T. landelsensis	4	125
T. podura	12	255
T. poppensis	5	116

243 Supplementary Table 2: Details of climate variables included in this study and loadings for the first three PCs
244 (Total proportion of variation explained by each PC: PC1 = 51.7%, PC2 = 24.4% and PC3 = 16.1%).

245

Code	Description	PC1	PC2	PC3
BIO1	Annual Mean Temperature	-0.24	0.21	0.15
BIO2	Mean Diurnal Range (Mean of monthly (max temp - min temp))	0.17	0.19	0.03
BIO3	Isothermality (BIO2/BIO7) (×100)	-0.22	-0.12	-0.24
BIO4	Temperature Seasonality (standard deviation ×100)	0.25	0.16	0.19
BIO5	Max Temperature of Warmest Month	0.06	0.33	0.31
BIO6	Min Temperature of Coldest Month	-0.29	0.03	0.04
BIO7	Temperature Annual Range (BIO5-BIO6)	0.25	0.19	0.17
BIO8	Mean Temperature of Wettest Quarter	-0.29	0.08	0.03
BIO9	Mean Temperature of Driest Quarter	-0.1	0.29	0.34
BIO10	Mean Temperature of Warmest Quarter	-0.02	0.34	0.33
BIO11	Mean Temperature of Coldest Quarter	-0.29	0.06	0.01
BIO12	Annual Precipitation	0.09	-0.32	0.31
BIO13	Precipitation of Wettest Month	0.02	-0.32	0.36
BIO14	Precipitation of Driest Month	0.26	-0.14	-0.04
BIO15	Precipitation Seasonality (Coefficient of Variation)	-0.25	-0.01	0.18
BIO16	Precipitation of Wettest Quarter	0.04	-0.31	0.36
BIO17	Precipitation of Driest Quarter	0.27	-0.06	-0.11
BIO18	Precipitation of Warmest Quarter	0.28	-0.05	-0.07
BIO19	Precipitation of Coldest Quarter	0.04	-0.32	0.34
Elev	Elevation	0.29	0	-0.02
Lat	Latitude	-0.19	-0.25	0.08
Long	Longitude	0.25	0.19	-0.02

Supplementary Table 3. Summary of model posterior predictive performance as approximated by the deviance information criterion (DIC) for models predicting parallelism as a function of genes and ecology. The full model in each case (for each PC) includes genes and ecology, and the null model includes only an intercept term. D gives the mean deviance and pD denotes the effective number of parameters. Lower DIC values denote better models. The best model for each PC is highlighted in bold.

PC	**Model**	**D**	**pD**	**DIC**
PC1	Full	51.03	12.17	63.2
	Genes	**52.04**	**11.03**	**63.1**
	Ecology	69.55	10.27	79.8
	Null	76.1	5	81.1
PC2	Full	81.38	4.95	86.3
	Genes	80.59	3.89	84.5
	Ecology	84.18	3.98	85.2
	Null	**80.48**	**2.85**	**83.3**
PC3	**Full**	**68.32**	**5.64**	**74**
	Genes	74.95	4.51	79.5
	Ecology	78.03	3.88	81.9
	Null	80.2	2.9	83.1

Supplementary Table 4. Excess overlap between top climate-associations windows and those where change was mostly strongly correlated with elevation in the release-recapture experiment. Results are shown for different top quantiles. Here 0.90 indicates the top 10% of windows, which corresponds to the results in the main text. We report the observed number of windows in the top quantiles for both change and climate association, the x-fold enrichment relative to null expectations, and the corresponding P-value for each PC climate variable. Results are shown for null distributions where all windows were permuted or randomized ("Full randomisation") and where randomisations were limited to windows with similar numbers of SNPs ("Constrained randomisation"). *P*-values ≤ .05 are highlighted in bold. Significant P-values denote whether the overlap is greater than expected by chance from a one-sided randomisation test.

PC1					
		Full randomisation		**Constrained randomisation**	
Quantile	**Observed**	**X-fold**	**P-value**	**X-fold**	**P-value**
0.9	108	1.40	**0.00001**	1.24	**0.005**
0.91	86	1.39	**0.0012**	1.19	**0.040**
0.92	75	1.53	**0.00021**	1.29	**0.014**
0.93	59	1.56	**0.00008**	1.29	**0.013**
0.94	48	1.72	**0.000012**	1.36	**0.014**
0.95	43	2.21	**0.00054**	1.65	**0.00012**
0.96	33	2.68	**0.0001**	1.84	**0.001**
0.97	25	3.58	**0.00032**	2.29	**0.0004**
0.98	15	4.83	**0.00002**	2.63	**0.001**
0.99	6	7.47	**0.00001**	3.07	0.14
PC2					
		Full randomisation		**Constrained randomisation**	
Quantile	**Observed**	**X-fold**	**P-value**	**X-fold**	**P-value**
0.9	101	1.32	**0.003**	1.21	**0.015**
0.91	77	1.24	**0.034**	1.12	0.138
0.92	67	1.37	**0.005**	1.21	0.062
0.93	53	1.39	**0.010**	1.22	0.064
0.94	44	1.59	**0.001**	1.32	**0.039**
0.95	36	1.86	**0.00043**	1.45	**0.014**
0.96	28	2.29	**0.000001**	1.66	**0.003**
0.97	17	2.48	**0.001**	1.64	**0.035**
0.98	9	2.92	**0.004**	1.57	0.122

0.99	2	2.58	0.180	1.15	0.534
PC3					
		Full randomisation		**Constrained randomisation**	
Quantile	**Observed**	**X-fold**	**P-value**	**X-fold**	**P-value**
0.9	105	1.37	**0.00021**	1.21	**0.021**
0.91	91	1.46	**0.00001**	1.27	**0.005**
0.92	73	1.48	**0.001**	1.27	**0.012**
0.93	50	1.32	**0.019**	1.11	0.232
0.94	40	1.45	**0.008**	1.17	0.157
0.95	26	1.33	0.068	1.04	0.438
0.96	20	1.60	**0.027**	1.22	0.188
0.97	12	1.72	**0.049**	1.25	0.264
0.98	5	1.68	0.188	1.04	0.516
0.99	3	3.95	0.028	2.50	0.103

Supplementary Table 5. Bayesian estimates of the percent of CHC variation explained by sequenced SNPs. Estimates are from the polygenic GWA in gemma. The posterior median gives the point estimate of the percent of CHC variation explained by the SNPs; the 95% equal-tail probability intervals (ETPIs) are also given.

Trait	**Posterior median**	**95% ETPI**
Female pentacosanes	89.7	35.8-99.9
Female heptacosanes	52.5	4.9-98.9
Female nonacosanes	80.2	15.5-99.8
Male pentacosanes	53.2	8.3-97.2
Male heptacosanes	52.4	10.3-96.5
Male nonacosanes	50.8	7.8-95.6

Supplementary Table 6: X-fold enrichments and associated *P*-values for number of overlapping SNP windows for PC1 for comparison with genetic mapping of CHCs. Observed value gives the mean posterior inclusions probability (i.e., probability of a genotype-phenotype association) across all SNPs in 100 Kb windows for each of the six CHC traits. *P*-values ≤ .05 are highlighted in bold. Significant P-values denote whether the overlap is greater than expected by chance from a one-sided randomisation test.

T. bartmani				***T. podura***			
CHC	**X-fold**	**Observed**	***P*-value**	**CHC**	**X-fold**	**Observed**	***P*-value**
F-penta	1.06	0.000439	0.128	F-penta	1.07	0.0004425	0.059
F-hepta	1.02	0.000301	0.271	F-hepta	1.01	0.0002928	0.457
F-nona	0.99	0.000264	0.526	F-nona	0.94	0.00024994	0.909
M-penta	0.96	0.000345	0.781	M-penta	0.99	0.00035676	0.551
M-hepta	1.07	0.000508	0.072	M-hepta	1.03	0.00048354	0.265
M-nona	0.9	0.000325	0.576	M-nona	0.98	0.00032352	0.641
T. chumash				***T. cristinae***			
CHC	**X-fold**	**Observed**	***P*-value**	**CHC**	**X-fold**	**Observed**	***P*-value**
F-penta	0.89	0.00036706	0.983	F-penta	1.01	0.00041936	0.217
F-hepta	0.94	0.00027501	0.898	F-hepta	1.01	0.00029503	0.266
F-nona	0.98	0.00025862	0.674	F-nona	0.94	0.00024953	0.997
M-penta	0.99	0.00035754	0.512	M-penta	0.99	0.0003586	0.509
M-hepta	0.97	0.00045792	0.712	M-hepta	0.95	0.00044654	0.992
M-nona	1.06	0.00034639	0.122	M-nona	0.97	0.00031857	0.942
T. knulli				***T. poppensis***			
CHC	**X-fold**	**Observed**	***P*-value**	**CHC**	**X-fold**	**Observed**	***P*-value**
F-penta	0.96	0.00039798	0.859	F-penta	0.98	0.00040417	0.689
F-hepta	1.02	0.00029934	0.201	F-hepta	0.99	0.00029192	0.521
F-nona	1.03	0.00027378	0.132	F-nona	0.96	0.00025463	0.856
M-penta	1.02	0.00036701	0.232	M-penta	1	0.00036056	0.429
M-hepta	0.99	0.00046794	0.554	M-hepta	1.03	0.00048384	0.208
M-nona	1	0.00033049	0.465	M-nona	1.07	0.00035128	**0.024**
T. landelsensis				***T. californicum***			
CHC	**X-fold**	**Observed**	***P*-value**	**CHC**	**X-fold**	**Observed**	***P*-value**
F-penta	0.94	0.00039035	0.951	F-penta	0.97	0.00040217	0.753
F-hepta	0.98	0.00028747	0.684	F-hepta	0.99	0.00028878	0.601
F-nona	0.97	0.00025692	0.819	F-nona	0.98	0.00026206	0.625
M-penta	0.98	0.00035169	0.726	M-penta	0.96	0.00034453	0.892
M-hepta	1.03	0.00048427	0.201	M-hepta	1.05	0.00049524	0.071
M-nona	1.02	0.00033471	0.304	M-nona	1.01	0.00033312	0.333

Supplementary Table 7: X-fold enrichments and associated *P*-values for number of overlapping SNP windows for PC2 for comparison with CHC experiment. Observed value gives the mean posterior inclusions probability (i.e., probability of a genotype-phenotype association) across all SNPs in 100 Kb windows for each of the six CHC traits. *P*-values ≤ .05 are highlighted in bold. Significant P-values denote whether the overlap is greater than expected by chance from a one-sided randomisation test.

T. bartmani				***T. podura***			
CHC	**X-fold**	**Observed**	***P*-value**	**CHC**	**X-fold**	**Observed**	***P*-value**
F-penta	0.97	0.000403	0.681	F-penta	0.99	0.00041351	0.486
F-hepta	1.05	0.000306	0.143	F-hepta	0.92	0.00027053	0.978
F-nona	1	0.000265	0.494	F-nona	1.06	0.00028006	0.089
M-penta	0.96	0.000345	0.773	M-penta	0.97	0.00035019	0.709
M-hepta	0.96	0.000455	0.734	M-hepta	1.05	0.00049492	0.113
M-nona	0.99	0.000326	0.573	M-nona	0.89	0.0002953	0.994
T. chumash				***T. cristinae***			
CHC	**X-fold**	**Observed**	***P*-value**	**CHC**	**X-fold**	**Observed**	***P*-value**
F-penta	1.01	0.00041693	0.417	F-penta	1.05	0.0004352	**0.009**
F-hepta	0.95	0.00027777	0.863	F-hepta	0.98	0.00028726	0.805
F-nona	1.04	0.00027621	0.191	F-nona	1.01	0.00026784	0.286
M-penta	1.05	0.00037559	0.172	M-penta	1.01	0.00036299	0.286
M-hepta	0.98	0.00046092	0.628	M-hepta	0.96	0.00045164	0.976
M-nona	0.92	0.00030343	0.955	M-nona	0.99	0.00032555	0.681
T. knulli				***T. poppensis***			
CHC	**X-fold**	**Observed**	***P*-value**	**CHC**	**X-fold**	**Observed**	***P*-value**
F-penta	1.02	0.00041785	0.295	F-penta	1.03	0.00042699	0.171
F-hepta	1.02	0.00029805	0.221	F-hepta	1.04	0.0003051	0.087
F-nona	0.98	0.00025978	0.738	F-nona	0.97	0.00025664	0.811
M-penta	0.97	0.00034943	0.806	M-penta	1.06	0.0003824	**0.042**
M-hepta	0.99	0.00046472	0.612	M-hepta	1.05	0.00049262	0.093
M-nona	1	0.00032921	0.471	M-nona	0.97	0.00032084	0.772
T. landelsensis				***T. californicum***			
CHC	**X-fold**	**Observed**	***P*-value**	**CHC**	**X-fold**	**Observed**	***P*-value**
F-penta	0.92	0.00038096	0.987	F-penta	0.95	0.00039456	0.895
F-hepta	0.97	0.0002817	0.864	F-hepta	0.93	0.00027181	0.99
F-nona	1.01	0.00026628	0.43	F-nona	1.01	0.00026813	0.346
M-penta	0.99	0.00035724	0.517	M-penta	1.05	0.00037699	0.062
M-hepta	1.01	0.00047379	0.437	M-hepta	1.01	0.00047356	0.395
M-nona	0.99	0.00032686	0.561	M-nona	0.96	0.00031934	0.831

Supplementary Table 8: X-fold enrichments and associated *P*-values for number of overlapping SNP windows for PC3 for comparison with CHC experiment. Observed value gives the mean posterior inclusions probability (i.e., probability of a genotype-phenotype association) across all SNPs in 100 Kb windows for each of the six CHC traits. *P*-values ≤ .05 are highlighted in bold. Significant P-values denote whether the overlap is greater than expected by chance from a one-sided randomisation test.

T. bartmani				***T. podura***			
CHC	**X-fold**	**Observed**	***P*-value**	**CHC**	**X-fold**	**Observed**	***P*-value**
F-penta	1.06	0.000439	0.128	F-penta	1.03	0.00042715	0.222
F-hepta	1.02	0.000301	0.271	F-hepta	1.04	0.00030464	0.132
F-nona	0.99	0.000264	0.526	F-nona	0.93	0.00024736	0.948
M-penta	0.96	0.000345	0.781	M-penta	1.08	0.00038877	**0.029**
M-hepta	1.07	0.000508	0.072	M-hepta	1.09	0.00051268	**0.028**
M-nona	0.9	0.000325	0.576	M-nona	0.99	0.00032619	0.531
T. Chumash				***T. cristinae***			
CHC	**X-fold**	**Observed**	***P*-value**	**CHC**	**X-fold**	**Observed**	***P*-value**
F-penta	1.07	0.0004442	0.088	F-penta	1.05	0.00043482	**0.012**
F-hepta	0.99	0.0002889	0.569	F-hepta	1.01	0.00029312	0.393
F-nona	0.94	0.00024939	0.889	F-nona	1.03	0.00027351	0.051
M-penta	1.03	0.00037132	0.216	M-penta	0.99	0.00035579	0.666
M-hepta	1.03	0.00048255	0.281	M-hepta	0.98	0.00046005	0.832
M-nona	1.05	0.00034602	0.164	M-nona	0.98	0.00032394	0.791
T. knulli				***T. poppensis***			
CHC	**X-fold**	**Observed**	***P*-value**	**CHC**	**X-fold**	**Observed**	***P*-value**
F-penta	1.05	0.00043564	0.054	F-penta	1.06	0.00043928	**0.034**
F-hepta	0.99	0.0002911	0.547	F-hepta	0.97	0.00028301	0.832
F-nona	0.97	0.00025644	0.842	F-nona	0.96	0.00025389	0.894
M-penta	1.03	0.00036955	0.141	M-penta	0.93	0.00033533	0.981
M-hepta	0.99	0.00046841	0.563	M-hepta	0.98	0.0004604	0.723
M-nona	0.99	0.00032395	0.676	M-nona	0.96	0.00031526	0.903
T. landelsensis				***T. californicum***			
CHC	**X-fold**	**Observed**	***P*-value**	**CHC**	**X-fold**	**Observed**	***P*-value**
F-penta	1.03	0.0004247	0.236	F-penta	1.02	0.0004232	0.268
F-hepta	1.03	0.00030062	0.175	F-hepta	0.95	0.00027931	0.913
F-nona	0.99	0.00026403	0.532	F-nona	0.97	0.00026	0.732
M-penta	0.97	0.00034978	0.769	M-penta	0.98	0.00035164	0.713
M-hepta	0.95	0.00044452	0.939	M-hepta	1.05	0.00049509	0.068
M-nona	1.05	0.00034642	0.056	M-nona	0.99	0.00032631	0.594

Supplementary Table 9: Proportion of variation explained by the TREEMIX [8] population graph with different numbers of migration edges.

Number of migration edges	Proportion of variation explained
0	0.997
1	0.998
2	0.998
3	0.998
4	0.999
5	0.999
6	0.999
7	0.999
8	0.999
9	0.999

SUPPLEMENTARY FIGURES

SUPPLEMENTARY FIGURES 1, 2, 3: Plots shows parameter estimates with standardized coefficients for the full model for PC1, PC2, and PC3 for the permuted data sets compared to the original data set. The PC variables were randomized before running BayPass. This test was implemented for all eight species and 56 species pairs. Here the gray points denote estimates for permuted data sets, and red points indicate estimates of original data. Gray lines indicate 95% equal-tail probability intervals (ETPIs). Estimates diverging from zero indicate a positive or negative effect of ecology or genetics on parallelism.

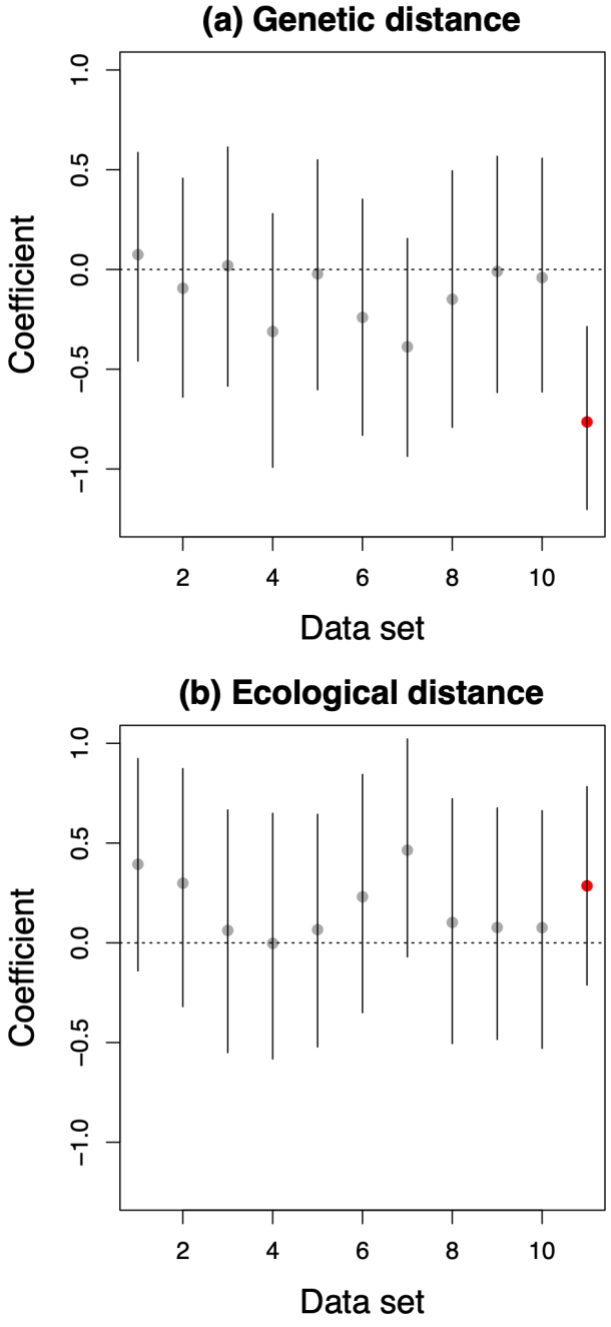

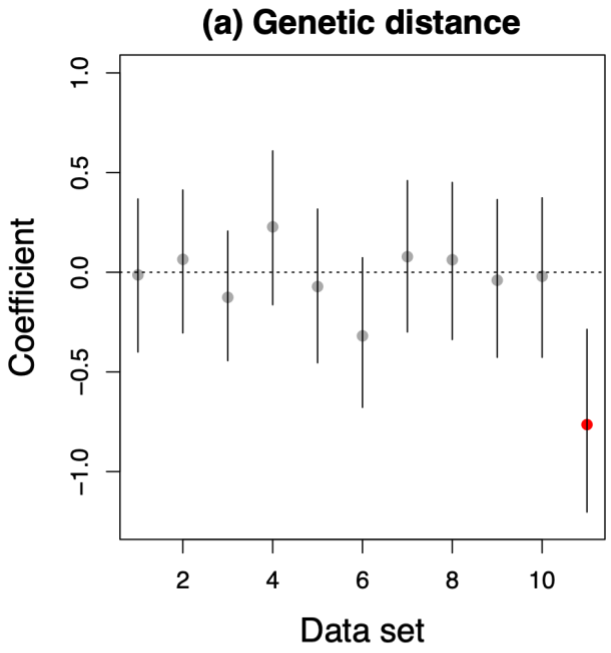
(a) Genetic distance
Coefficient
1.0
0.5
0.0
−0.5
−1.0
2
4
6
8
10
Data set

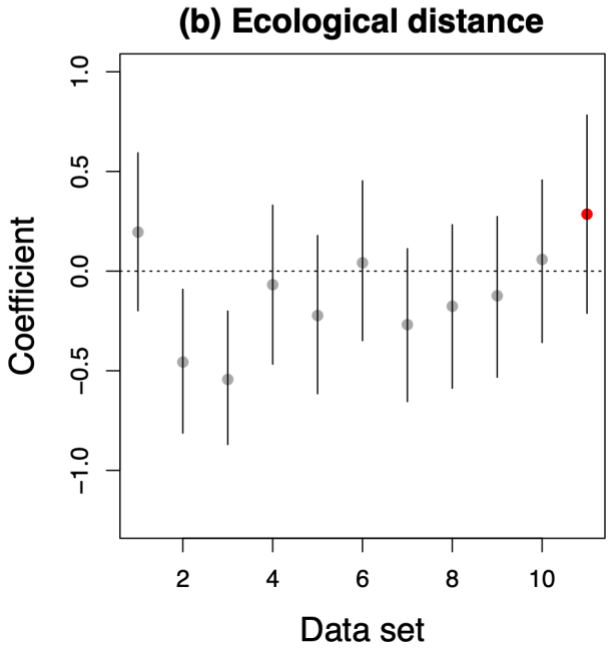
(b) Ecological distance
Coefficient
1.0
0.5
0.0
−0.5
−1.0
2
4
6
8
10
Data set

310

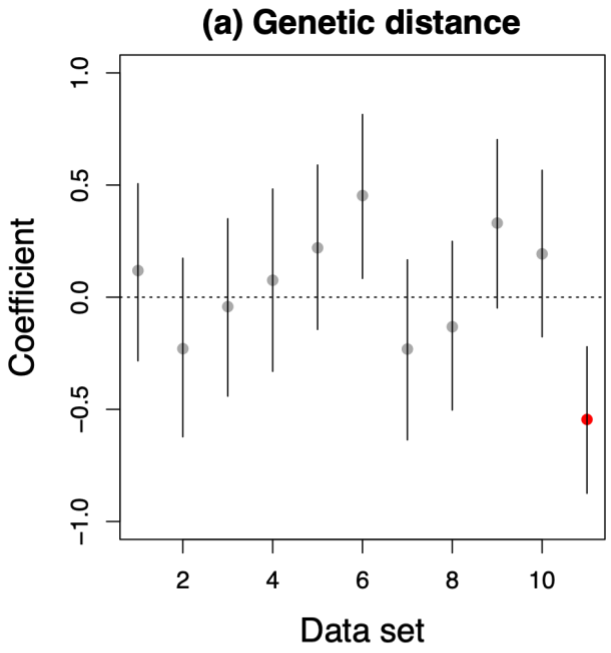
(a) Genetic distance
Coefficient
1.0
0.5
0.0
−0.5
−1.0
2
4
6
8
10
Data set

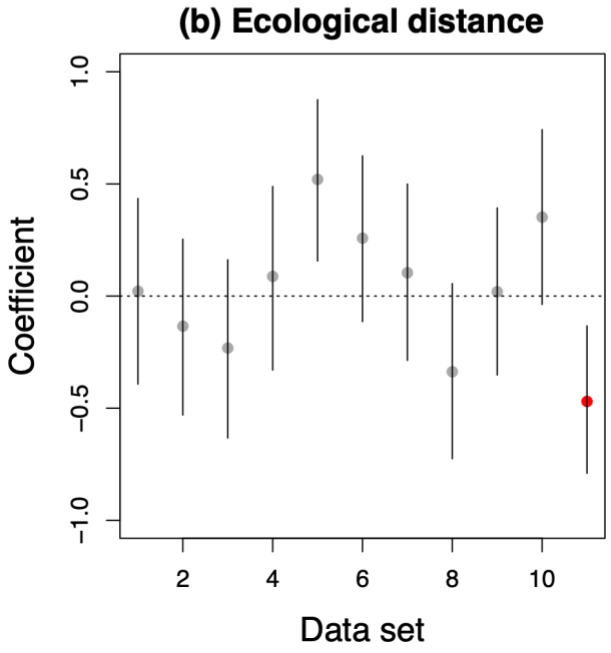
(b) Ecological distance
Coefficient
1.0
0.5
0.0
−0.5
−1.0
2
4
6
8
10
Data set

311

SUPPLEMENTARY FIGURE 4: Tests for parallel climate-associated SNP windows between species of *Timema* stick insects (all plots are for the top 10% empirical quantile) using randomized PC1 variables before running BayPass. Bars denote the x-fold enrichments for the number of overlapping climate-associated SNP windows for PC1 for multi-species comparisons between 2 or more, 3 or more, and 4 or more species generated in the randomisations. N values above each bar indicate the number of overlapping climate-associated SNP windows for each comparison in the randomisations. Red dot above each bar indicates the x-fold enrichment for each comparison determined for the original dataset. * Indicates x-fold enrichments of permuted data sets with P-value < 0.05.

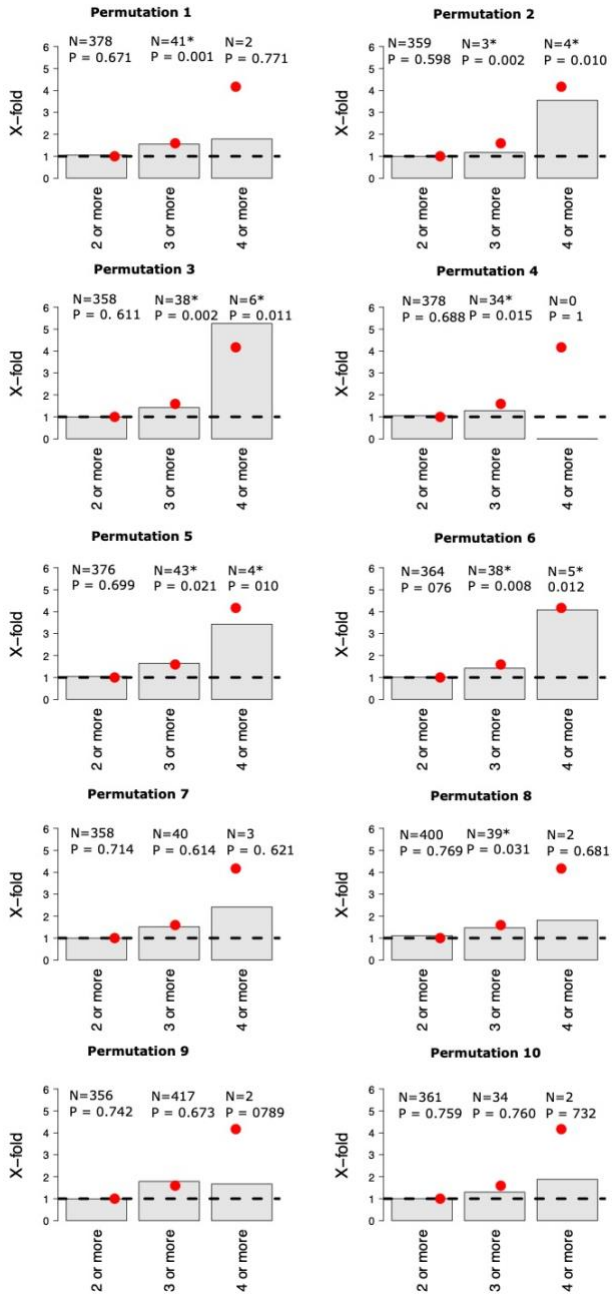

SUPPLEMENTARY FIGURE 5: Tests for parallel climate-associated SNP windows between species of *Timema* stick insects (all plots are for the top 10% empirical quantile) using randomized PC2 variables before running BayPass. Bars denote the x-fold enrichments for the number of overlapping climate-associated SNP windows for PC2 for multi-species comparisons between 2 or more, 3 or more, and 4 or more species generated in the randomisations. N values above each bar indicate the number of overlapping climate-associated SNP windows for each comparison in the randomisations. Red dot above each bar indicates the x-fold enrichment for each comparison determined for the original dataset. * Indicates x-fold enrichments of permuted data sets with P- value ≤ 0.05.

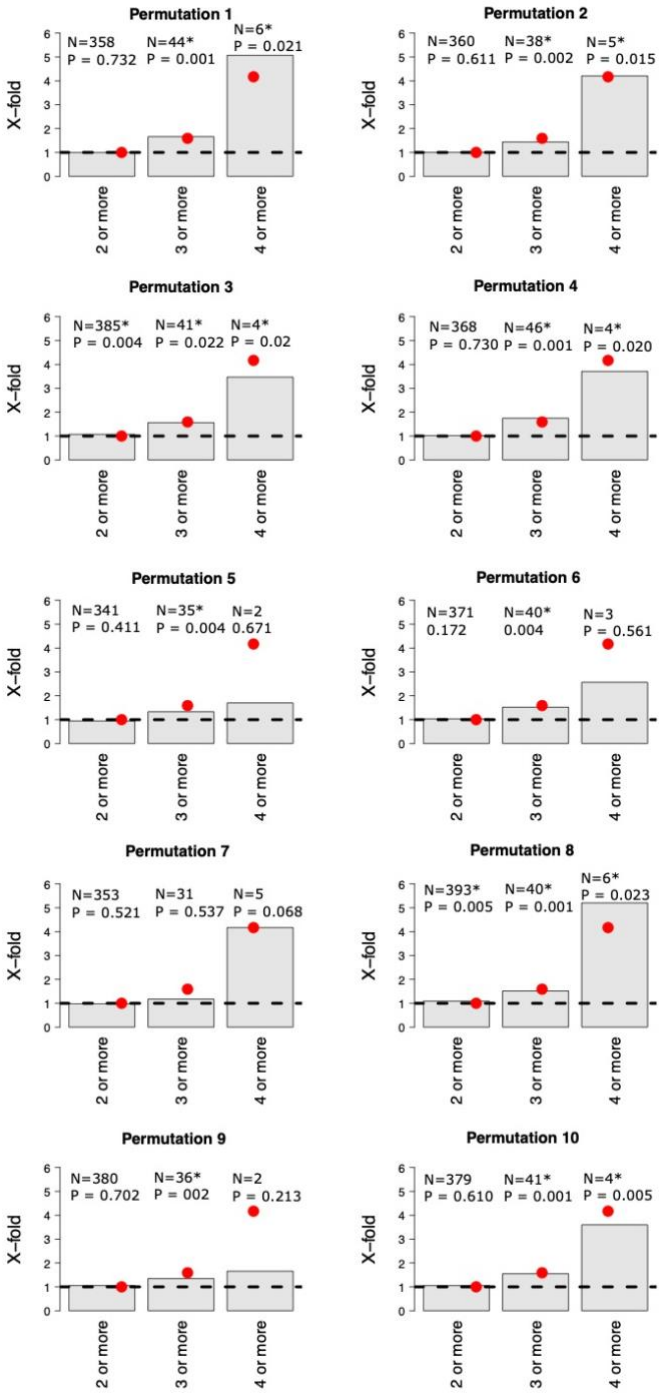

.

SUPPLEMENTARY FIGURE 6: Tests for parallel climate-associated SNP windows between species of *Timema* stick insects (all plots are for the top 10% empirical quantile) using randomized PC3 variables before running BayPass. Bars denote the x-fold enrichments for the number of overlapping climate-associated SNP windows for PC3 for multi-species comparisons between 2 or more, 3 or more, and 4 or more species generated in the randomisations. N values above each bar indicate the number of overlapping climate-associated SNP windows for each comparison in the randomisations. Red dot above each bar indicates the x-fold enrichment for each comparison determined for the original dataset. * Indicates x-fold enrichments of permuted data sets with P-value ≤ 0.05.

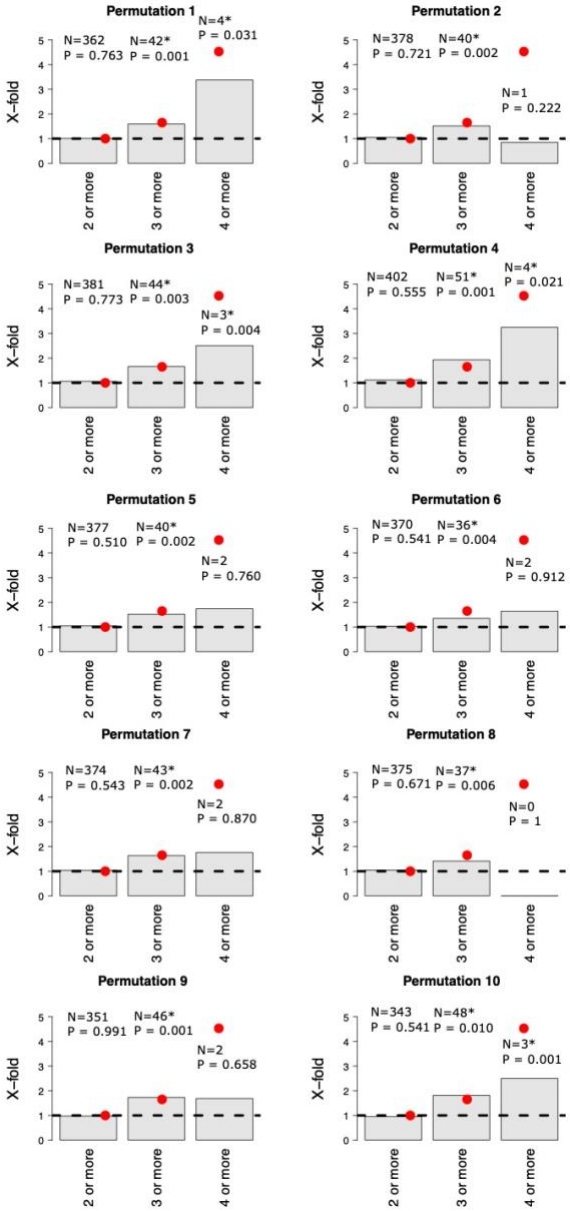

SUPPLEMENTARY FIGURES 7, 8, 9: Plots show summaries of population structure based on principal component analysis for eight species included in this study for PC1 vs. PC2 (Supplementary Figure 7), PC1 vs. PC3 (Supplementary Figure 8), and PC2 vs. PC3 (Supplementary Figure 9). Abbreviations indicate populations corresponding to SUPPLEMENTARY TABLE 1.

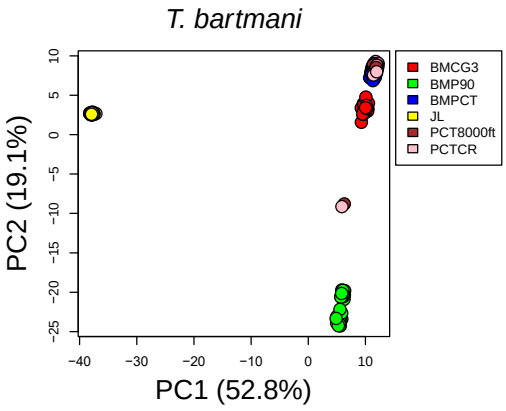
T. bartmani
PC2 (19.1%)
PC1 (52.8%)
BMCG3
BMP90
BMPCT
JL
PCT8000ft
PCTCR

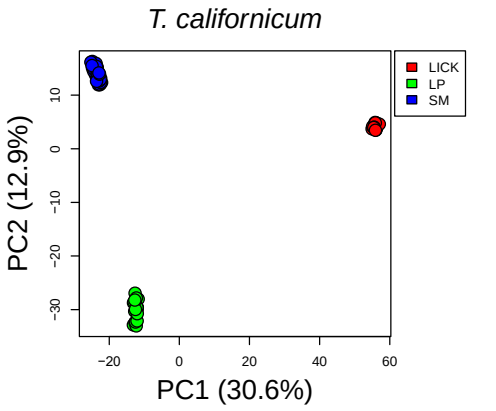
T. californicum
PC2 (12.9%)
PC1 (30.6%)
LICK
LP
SM

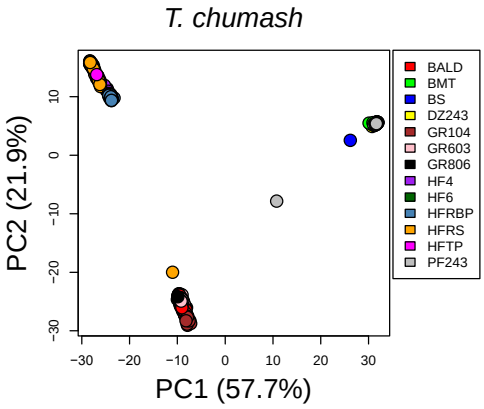
T. chumash
PC2 (21.9%)
PC1 (57.7%)
BALD
BMT
BS
DZ243
GR104
GR603
GR806
HF4
HF6
HFRBP
HFRS
HFTP
PF243

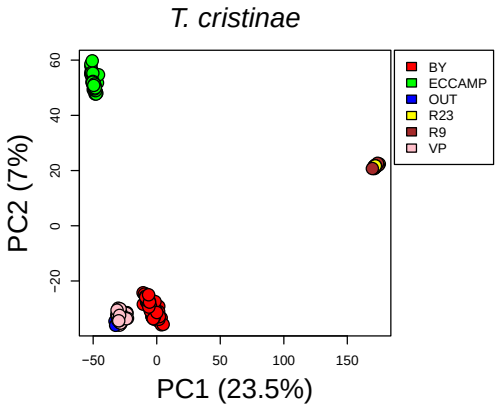
T. cristinae
PC2 (7%)
PC1 (23.5%)
BY
ECCAMP
OUT
R23
R9
VP

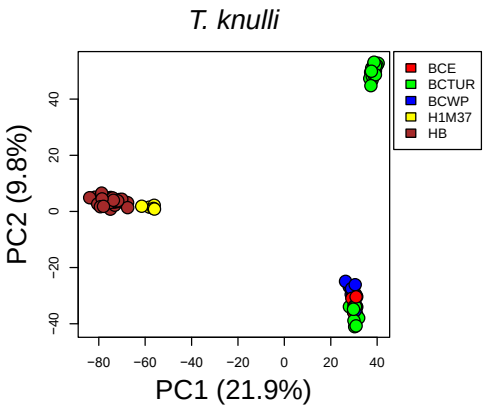
T. knulli
PC2 (9.8%)
PC1 (21.9%)
BCE
BCTUR
BCWP
H1M37
HB

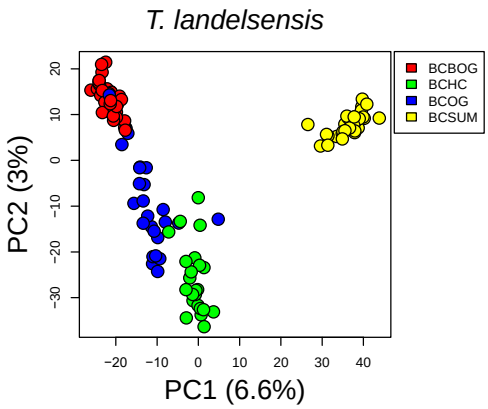
T. landelsensis
PC2 (3%)
PC1 (6.6%)
BCBOG
BCHC
BCOG
BCSUM

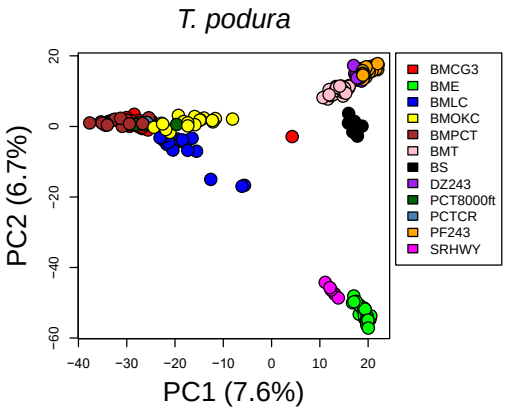
T. podura
PC2 (6.7%)
PC1 (7.6%)
BMCG3
BME
BMLC
BMOKC
BMPCT
BMT
BS
DZ243
PCT8000ft
PCTCR
PF243
SRHWY

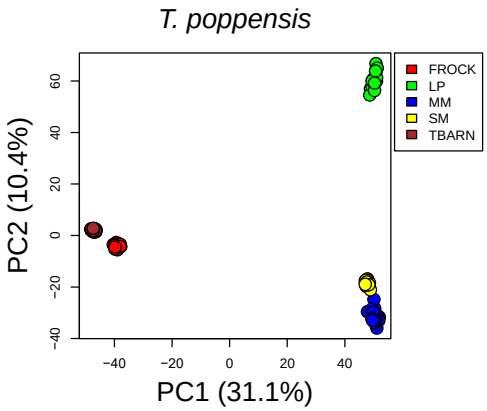
T. poppensis
PC2 (10.4%)
PC1 (31.1%)
FROCK
LP
MM
SM
TBARN

349

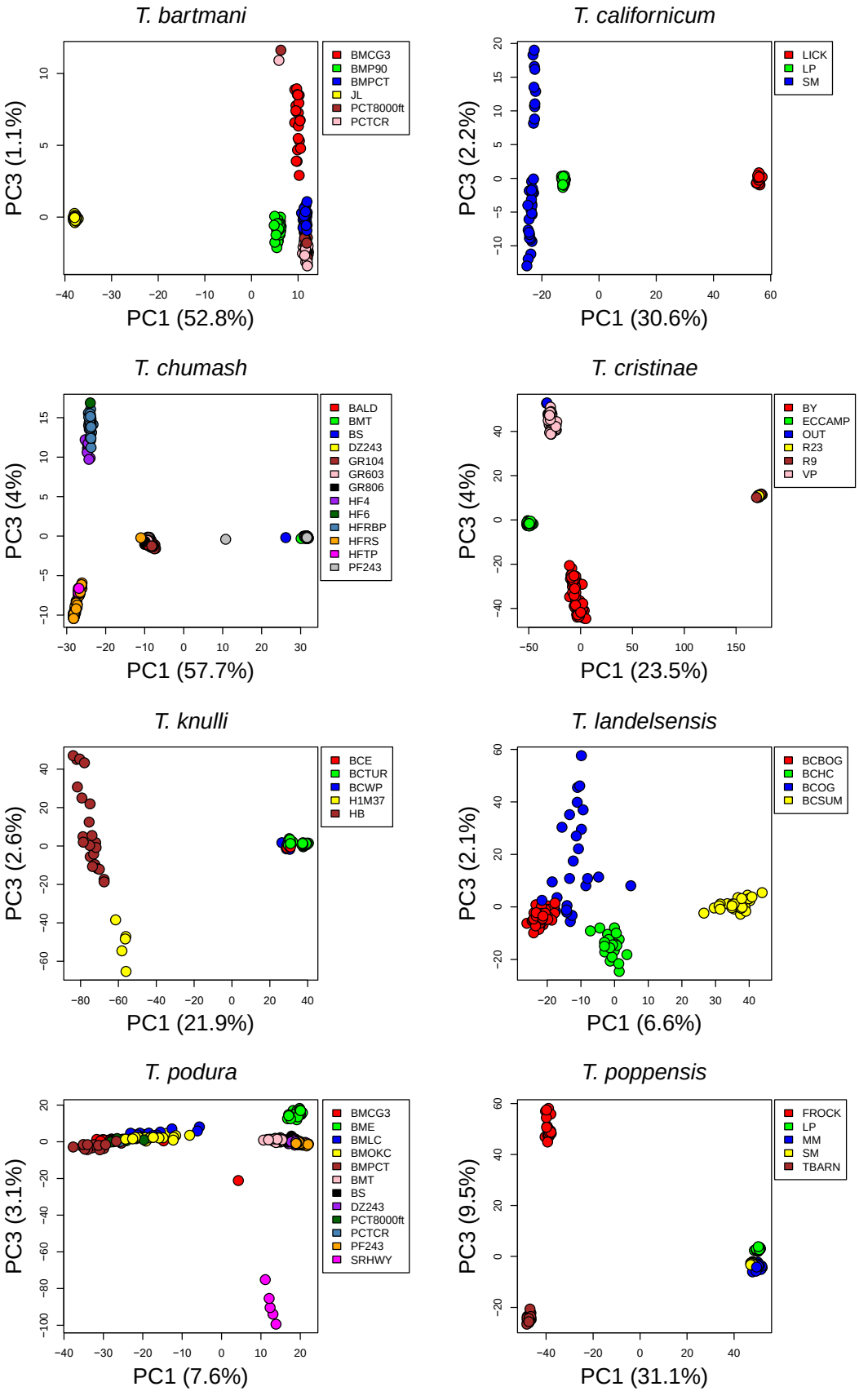
T. bartmani
BMCG3
BMP90
BMPCT
JL
PCT8000ft
PCTCR
PC3 (1.1%)
PC1 (52.8%)
T. californicum
LICK
LP
SM
PC3 (2.2%)
PC1 (30.6%)
T. chumash
BALD
BMT
BS
DZ243
GR104
GR603
GR806
HF4
HF6
HFRBP
HFRS
HFTP
PF243
PC3 (4%)
PC1 (57.7%)
T. cristinae
BY
ECCAMP
OUT
R23
R9
VP
PC3 (4%)
PC1 (23.5%)
T. knulli
BCE
BCTUR
BCWP
H1M37
HB
PC3 (2.6%)
PC1 (21.9%)
T. landelsensis
BCBOG
BCHC
BCOG
BCSUM
PC3 (2.1%)
PC1 (6.6%)
T. podura
BMCG3
BME
BMLC
BMOKC
BMPCT
BMT
BS
DZ243
PCT8000ft
PCTCR
PF243
SRHWY
PC3 (3.1%)
PC1 (7.6%)
T. poppensis
FROCK
LP
MM
SM
TBARN
PC3 (9.5%)
PC1 (31.1%)

350

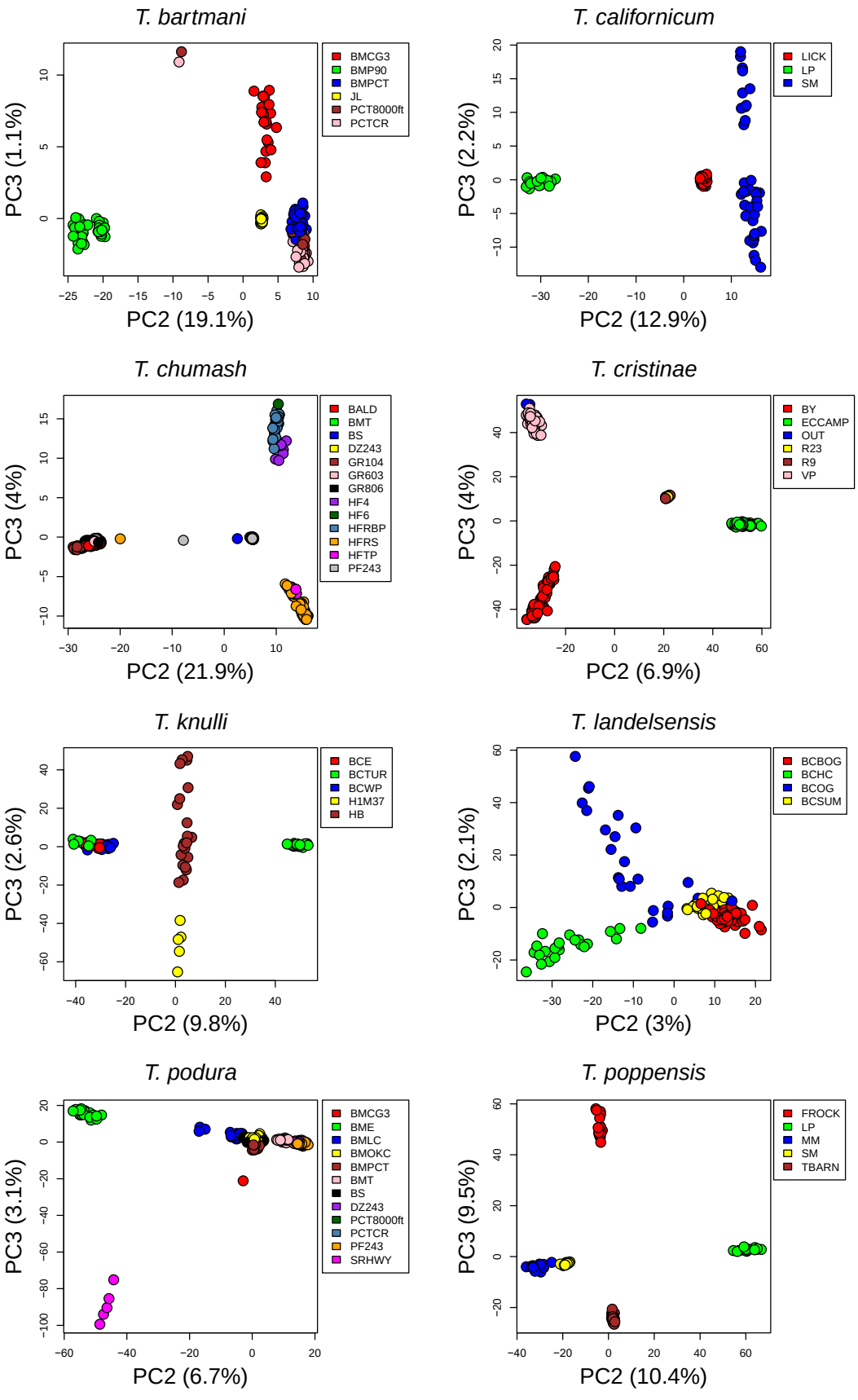
T. bartmani
PC3 (1.1%)
PC2 (19.1%)
BMCG3
BMP90
BMPCT
JL
PCT8000ft
PCTCR
T. californicum
PC3 (2.2%)
PC2 (12.9%)
LICK
LP
SM
T. chumash
PC3 (4%)
PC2 (21.9%)
BALD
BMT
BS
DZ243
GR104
GR603
GR806
HF4
HF6
HFRBP
HFRS
HFTP
PF243
T. cristinae
PC3 (4%)
PC2 (6.9%)
BY
ECCAMP
OUT
R23
R9
VP
T. knulli
PC3 (2.6%)
PC2 (9.8%)
BCE
BCTUR
BCWP
H1M37
HB
T. landelsensis
PC3 (2.1%)
PC2 (3%)
BCBOG
BCHC
BCOG
BCSUM
T. podura
PC3 (3.1%)
PC2 (6.7%)
BMCG3
BME
BMLC
BMOKC
BMPCT
BMT
BS
DZ243
PCT8000ft
PCTCR
PF243
SRHWY
T. poppensis
PC3 (9.5%)
PC2 (10.4%)
FROCK
LP
MM
SM
TBARN

351